Metabolic Brain Disease (2019) 34:1365–1374
https://doi.org/10.1007/s11011-019-00447-8

ORIGINAL ARTICLE

Amyloid Beta 25–35 induces blood-brain barrier disruption in vitro

Elvis Cuevas[1] · Hector Rosas-Hernandez[1] · Susan M. Burks[1] · Manuel A. Ramirez-Lee[1] · Aida Guzman[2] · Syed Z. Imam[1] · Syed F. Ali[1] · Sumit Sarkar[1]

Received: 13 September 2018 / Accepted: 5 June 2019 / Published online: 2 July 2019

Abstract

The amyloid β-peptide (Aβ) is transported across the blood-brain barrier (BBB) by binding with the receptor for advanced glycation end products (RAGE). Previously, we demonstrated that the Aβ fraction 25–35 ($Aβ_{25–35}$) increases RAGE expression in the rat hippocampus, likely contributing to its neurotoxic effects. However, it is still debated if the interaction of Aβ with RAGE compromises the BBB function in Alzheimer' disease (AD). Here, we evaluated the effects of $Aβ_{25–35}$ in an established in vitro model of the BBB. Rat brain microvascular endothelial cells (rBMVECs) were treated with 20 μM active $Aβ_{25–35}$ or the inactive $Aβ_{35–25}$ (control), for 24 h. Exposure to $Aβ_{25–35}$ significantly decreased cell viability, increased cellular necrosis, and increased the production of reactive oxygen species (ROS), which triggered a decrease in the enzyme glutathione peroxidase when compared to the control condition. $Aβ_{25–35}$ also increased BBB permeability by altering the expression of tight junction proteins (decreasing zonula occludens-1 and increasing occludin). $Aβ_{25–35}$ induced monolayer disruption and cellular disarrangement of the BBB, with RAGE being highly expressed in the zones of disarrangement. Together, these data suggest that $Aβ_{25–35}$-induces toxicity by compromising the functionality and integrity of the BBB in vitro.

Keywords Amyloid β fraction 25–35 · Blood-brain barrier · Oxidative stress · Permeability · RAGE · Zonula occludens 1

Introduction

Alzheimer's disease (AD) is a common neurodegenerative disorder in the elderly, which results in a progressive loss of cognitive function (Alzheimer's 2016). While the relationship between AD pathology and symptomology has not been fully defined, overproduction and accumulation of the amyloid β-peptide (Aβ) is a hallmark pathological feature of AD (Hardy and Selkoe 2002; Selkoe and Hardy 2016). It is likely that pathological Aβ processing is related to symptom severity (Thal et al. 2002). Overtime, the excessive accumulation of Aβ peptides in different stages of aggregation, predominantly within the neocortex, will develop into neuritic plaques (NPs) (Hardy and Allsop 1991; Hardy and Selkoe 2002; Steinerman et al. 2008). While rare familial forms of the AD are characterized by increased production of Aβ, it is postulated that a decrease in Aβ clearance from the brain might be crucial to the pathology observed in the more common sporadic type of AD (Mawuenyega et al. 2010). Several mechanisms function in synchronization to effectively clear Aβ from the brain, with the most prominent being active transport across the blood-brain barrier (BBB) (Weller et al. 2008).

The BBB plays an important role in the homeostasis of Aβ brain levels, and dysfunction of the BBB may contribute to the pathogenesis of AD (Deane and Zlokovic 2007; Do et al. 2016). As its name suggests, the primary role of the BBB is to serve as a barrier and filter to regulate influx of substances to the brain. The integrity of the BBB is maintained by structural protein complexes called tight junctions (TJs). TJs are comprised of the scaffold protein zonula occludens-1 (ZO-1) (Watson et al. 1991) that directly binds to the transmembrane proteins claudin-5 (C-5) and occludin (OC) to the actin cytoskeleton (Fanning et al. 1998). These protein complexes are found in high abundance in the brain microvascular endothelium (Bednarczyk and Lukasiuk 2011). The high levels of TJs protein expression give the BBB its barrier-like properties and ability to restrict movement of various unwanted macromolecules from the blood to the brain (Mark and Davis 2002). By evaluating the effects of Aβ in various models of the BBB it

✉ Elvis Cuevas
Elvis-Yane.Cuevas-Martinez@fda.hhs.gov

[1] Division of Neurotoxicology, National Center for Toxicological Research/U.S. Food and Drug Administration, Jefferson, AR 72079, USA

[2] Escuela Nacional Preparatoria-UNAM, Mexico, Mexico

has been hypothesized that RAGE is responsible for transporting Aβ across the BBB to the brain. Conversely, low-density lipoprotein receptor-related protein 1 (LRP-1) (Mackic et al. 1998; Deane et al. 2003, 2004) appears to be responsible for transporting Aβ from the brain into the periphery. In addition, Aβ has been shown to disrupt the integrity of TJs (Strazielle et al. 2000); presumably by the interaction of Aβ and the receptor for advanced glycation end products (RAGE), which induces oxidative stress (OS) (Yan et al. 1996a, b; Kook et al. 2012). Together these finding suggest that the BBB may play a key role in the pathogenesis of AD.

It was demonstrated that Aβ25–35 possess similar activity like Aβ1–42, supporting that Aβ25–35 is a convenient model to evaluate the potential toxicity involved in the AD (Frozza et al. 2009). Importantly, $A\beta_{25–35}$ is physiologically present in elderly people, besides it has been found in AD postmortem brain patients (Millucci 2010; Kubo 2002). Our previous data indicated that microinjection of $A\beta_{25–35}$ into the rat hippocampus produced neurotoxicity, possibly via activation of the RAGE (Cuevas et al. 2011). As RAGE expression is increased in the brains of AD patients (Donahue et al. 2006; Deane 2012), it has been suggested that RAGE could interact with Aβ, mediating its transport across the BBB, thereby contributing to the formation of plaques that are typical in AD patients (Yan et al. 1996a, b; Wan et al. 2014b). Moreover, it has been suggested that the binding of Aβ to RAGE induces the activation of intracellular pathways that are involved in cell death, produces vascular dysfunction, decreases cerebral blood flow, and promotes neurovascular uncoupling and inflammatory reactions, all contributing to the progression of AD (Zlokovic 2011). Increased expression of RAGE, as well as its function as a ligand for Aβ, has prompted the scientific community to postulate that RAGE activation might contribute to BBB mediated AD-related pathology.

Despite evidence suggesting that RAGE plays a role in the Aβ-induced-toxicity to the BBB observed in the AD, little is known about the mechanisms of this toxicity, or the processes by which Aβ interacts with RAGE. It has been suggested that 16–23 residues of $A\beta_{1–40}$ binds to RAGE's V domain (Chaney et al. 2005; Xie et al. 2008; Gospodarska et al. 2011), but the binding of $A\beta_{25–35}$ to RAGE, and the consequences of this interaction has not been reported yet. The $A\beta_{25–35}$ fraction is the toxic domain of the Aβ and is used to mimic Aβ related toxicity in many molecular models of AD (Butterfield and Kanski 2002). The goal of this work is to explore the toxic interactions between $A\beta_{25–35}$ and the BBB, and to evaluate if RAGE is involved in these processes. To do this, we tested the effects of $A\beta_{25–35}$ using indicators of cell viability/damage; indicators of OS; indicators of the functionality and morphology of the rBMVEC as well as the localization of RAGE and Aβ in an in vitro BBB model. Through this approach we hope to begin to understand how RAGE and the BBB interact with Aβ to support AD pathogenesis.

Materials and methods

Primary cell culture

Ten brains per isolation were collected from adult male Wistar rats (380–420 g) obtained from the vivarium of the NCTR/FDA. All procedures with animals were carried out per the National Institutes of Health Guide for the Care and Use of Laboratory Animals. The animal protocol was approved by the NCTR/FDA Institutional Animal Care and Use Committee. rBMVECs were isolated using a modified method as previously described (Rosas-Hernandez et al. 2013a, b; 2018a, b). Briefly, the rBMEC were isolated from fresh rat brains, the cortex was dissected and treated with collagenase/dispase enzymes for digestion, finally, the rBMVEC separation was done by percoll gradient. The purity of the rBMEC has been demonstrated and standardized in our laboratory (Rosas-Hernandez et al. 2018a, b). Freshly isolated rBMVEC were plated (50,000 cells/cm^2) on collagen-coated and fibronectin-treated 96 well (MTT, LDH, ROS assays), 6 well (WB and histology analysis), or 6 well trans-well (TEER and permeability assays) plates in complete media (45% MEM, 45% Ham's F-12 nutrient mix, 10 mM HEPES, 13 mM sodium bicarbonate, 50 μg/cm^3 gentamicin, 20% FBS, 2.0 μg/cm^3 amphotericin B, and 100 μg/cm^3 sodium heparin) and incubated in a humidified incubator (37 °C, 5% CO_2). Heparin is a mitogen for endothelial cells and inhibits smooth cell and astrocyte growth. The cells were treated after 90% confluence was reached, typically at 10–12 days. However, in the case of 6 wells plates and trans-well plates, cells were treated after 100% confluence was reached, typically at 12–14 days. Three independent batches were isolated for the experiments.

Treatment of the cell monolayer

Synthetic $A\beta_{25–35}$ or $A\beta_{35–25}$ were purchased from SIGMA (A4559 and A2201, San Luis Missouri, USA). Aβ25–35 or Aβ35–25 peptides were reconstituted at 1 mM following manufacture specifications, then aliquoted (100 μL) and stored (-80 °C). The stocks peptides solutions were diluted with the cell media at 100 μM, and were incubated at 37 °C for 24 h prior to its use, since it has been proved that under these conditions is toxic (Pike et al. 1993; Pike et al. 1995; Frozza et al. 2009). The reverse peptide, $A\beta_{35–25}$, has been previously used as a control to test the effects of the $A\beta_{25–35}$ peptide (Self et al. 2005), because $A\beta_{35–25}$ lacks of aggregation (Park et al. 2013), did not produce any significant cellular proliferation changes comparing with neutral conditions (Stepanichev et al. 2010), these properties make $A\beta_{35–25}$ a suitable per se control for $A\beta_{25–35}$. All the cell treatments were performed for 24 h. The 20 μM concentration was selected based on previous studies showing that nanomolar

concentrations are neurotrophic and micromolar concentrations are neurotoxic (especially after 10 μM) (Yankner et al. 1990; Zheng et al. 2014; Liu et al. 2017a). Upon 90% or 100% of confluence, rBMVECs were treated with $A\beta_{25–35}$ or $A\beta_{35–25}$ (control) at 20 μM, a set of experiments were done per isolation ($N = 3$ isolations, each isolation has at least triplicates per condition/per assay) independently. All assays were carried out 24 h after exposure to Aβ. All data represent the result of three independent experiments.

Cell viability assay

This is a colorimetric assay that measures the reduction of MTT to insoluble purple formazan, which is measured spectrophotometrically (Denizot and Lang 1986). Briefly, after 24 h of $A\beta_{25–35}$ or $A\beta_{35–25}$ treatment, rBMVEC media was removed and replaced with 100 μL of MTT (0.1 mg/mL) in assay media and incubated for 2 h. The solution was then aspirated, and propanol added to lyse the cells. Dishes were vigorously shaken for 1 min and the absorbance measured at 560 nm with 690 nm reference wavelength (SynergyMX, Biotek, Winooski, VT). In this assay a control (cell media) condition was included to evaluate the possible changes by $A\beta_{35–25}$, but not showed in the final graph. Data are expressed as percent of control.

Lactate dehydrogenase assay

The cellular lysis was tested using Cytotoxicity Detection Kit^{PLUS} (LDH, Roche). LDH activity was detected in media (2% FBS and phenol red-free) by manufacturer's specifications. Upon confluence, rBMVEC seeded in 96-well plates were treated with $A\beta_{25–35}$ or $A\beta_{35–25}$ for 24 h. Subsequently, 100 μL of the supernatant was transferred to a 96-well plate, the LDH reaction mixture (100 μL per well) added, the reaction incubated for 30 min under dark conditions, and the absorbance measured at 490 nm with a reference wavelength of 650 nm (Synergy MX, BioTek, Winooski, VT). In this assay a control (cell media) condition was included to evaluate the possible changes by $A\beta_{35–25}$, but not showed in the final graph. Data are expressed as percent of control.

Reactive oxygen species (ROS) assay

The ROS assay uses DCFH-DA (2′, 7′- di-chlorofluorescein di-acetate), as a result, intracellular DCF fluorescence can be used as an index to quantify the overall OS in cells (Wang and Joseph 1999). Briefly, DCFH-DA (200 μM) was added to exposure media containing Aβ treatments and the accumulation of DCF formation (fluorescence) was measured at an excitation wavelength of 485 nm and emission wavelength of 530 nm (Synergy MX, BioTek, Winooski, VT) after 24 h of $A\beta_{25–35}$ or $A\beta_{35–25}$ treatment. Data are expressed as the percentage of the intensity of fluorescence (DCF formation) with respect to control.

Transepithelial electric resistance (TEER) assay

As previously described (Rosas-Hernandez et al. 2013a, b), evaluation of TEER was performed with an epithelial volt/Ω meter (EVOM2, electrode STX2, World Precision Instruments, Inc. UK) to determine the integrity of the rBMVEC after $A\beta_{25–35}$ or $A\beta_{35–25}$ treatment. Cells had to achieve a TEER of 180 Ω to be considered confluent and suitable for further use in this assay. This happened when 100% confluence was reached, normally after 12–14 days. Measurements were done before (TEER initial) and after (TEER final) 24-h $A\beta_{25–35}$ or $A\beta_{35–25}$ exposure to establish the effect of treatment on monolayer integrity. Data are expressed as the percentage difference in TEER relative to control [Δ TEER (%)].

Permeability assay

This assay assesses the integrity of the rBMVEC monolayer, as indicated by tight-junction function, by measuring fluorescein flux (FF) (Rosas-Hernandez et al. 2013a, b). Measurements were done in permeability side-bi-side diffusion chambers (PermeGear, H-series, connected to heater/recirculator, run at 120v/500 rpm, PermeGear, Inc. USA). rBMVEC were seeded on 6 trans-well inserts and upon 100% confluency (TEER of 180 Ω), they were treated with either $A\beta_{25–35}$ or $A\beta_{35–25}$. After 24 h of treatment, the membrane of each well was excised and placed between the permeability chambers. FF from the apical to basolateral compartments was determined over 120 min after 10 μM concentration of fluorescein was added to the donor (apical side) compartment. The FF was quantified using a spectrofluorometer (excitation 485 nm, emission 530 nm; SynergyMX, Biotek), with increased fluorescence being inversely proportional to the integrity of the rBMVEC monolayer. Data were expressed in percentage FF with respect to control.

Western blot (WB) analysis

The protein expression of the OS related protein glutathione peroxidase (GPX-1/2), TJ proteins (ZO-1 and OC), and RAGE were measured by WB using a previously described immunoblotting method (Cuevas et al. 2010, Rosas-Hernandez et al. 2013a, b) after 24 h of either $A\beta_{25–35}$ or $A\beta_{35–25}$ exposure. Briefly, proteins from rBMVEC were extracted with RIPA buffer (Thermo Scientific) plus Halt protease and phosphatase inhibitor (1:100; Thermo Scientific), homogenized by ultrasonication for 10 s, and placed on ice on a shaker at 46.3×g for 15 min, followed by centrifugation at

14811.3×g at 4 °C for 20 min. Quantification of proteins was measured by bicinichoninic acid protein kit (Thermo Scientific). Electrophoresis was performed in Criterion precast gels by loading 40 μg of proteins (denatured and reduced at 95 °C with Laemmli buffer/beta-mercaptoethanol) into tris-glycine gels (4–20% Biorad) and running at 200 mV/65 min with running buffer. Proteins were then transferred from the gels to nitrocellulose membranes at 100 mV/30 min in the Trans-Blot® SD semi-dry transfer cell system (Bio-Rad). Membranes were blocked with 5% bovine serum albumin (Sigma, USA) and incubated with a combination the following: mouse anti-GPx1/2 (1:200, Santa Cruz, sc-133,160) goat anti-ZO-1 (1:500, Abcam, ab190085), mouse anti-Occludin, (OC, 1:500, Abcam, ab167161), or rabbit anti-RAGE (1:200, Thermo Scientific, PA1–075). Mouse anti-beta actin (βA,1:1000, Sigma, A5316) was used as a housekeeping protein (loading control). All primary antibodies were incubated overnight, and then secondary antibodies were added, either anti-mouse-HRP or anti-rabbit-HRP or anti-goat-HRP (1:1000, Jackson Immunoresearch), for 2 h at room temperature. Finally, detection was performed using an ECL detection kit (Thermoscientific) and Chemidoc XRS system (Bio-Rad). The digital images were analyzed with Image Studio software. βA quantifications were done in all the membranes after stripping to normalize levels of GPX1/2, ZO-1, OC, and RAGE. Results were expressed in integrated density ratio of GPX/, ZO-1/, OC/, RAGE/βA.

The data collected, from the densitometry analysis, was from tree different isolations ($N = 3$). The number of replicates varies depending on the yield of cells on each isolation. The main criteria, in terms of statistical analysis, was having at least 3 replicates per isolation. The actual values represent the average of all the replicates from at least 3 separate isolation per each condition. The final figure for each protein target was done using the most representative band for each condition.

Morphological analysis and immunofluorescence

To check the cellular arrangement and localization of Aβ and RAGE, morphological analysis was performed with conventional light or fluorescence microscopy (Nikon Eclipse Ti, software NIS-Elements AR 3.10). The rBMVEC cells were grown on cover-slips in 6-well (Costar) chambers for all the histological analysis. Once the cells reached confluence, cells were exposed with either $A\beta_{25–35}$ or $A\beta_{35–25}$. After 24 h of exposure, cells were fixed in 4% paraformaldehyde in PBS pH 7.4 for 15 min. Pictures were taken under conventional light for the overview of the cellular arrangement at 10X. To assess the colocalization of Aβ with RAGE, after fixation, cells were blocked with 5% bovine serum albumin (Sigma, USA) and incubated with rabbit anti-RAGE (1:200, Thermo Scientific, PA1–075) and mouse anti-Aβ40/42 (1:200, Biosensis, M-1586-100). After overnight incubation at 4 °C, the corresponding secondary antibodies were added [anti-rabbit- FITC or anti-mouse- CY3 (1:500, Jackson Immunoresearch)] and incubation occurred for 2 h at room temperature. Pictures were taken with a fluorescent microscope (Nikon Eclipse Ni, software NIS-Elements 4.20.00), at 10X. Digital images were analyzed for the quantification of the intensity of labeling, using Image J_NIH software. Results were expressed in intensity percent of control.

Statistical analysis

All data are expressed as mean values ± SEM and were analyzed using Student "t" test. All statistical analyses were performed using GraphPad Prism 6 software (GraphPad Scientific, San Diego, CA, USA). Differences of *p*-values below 0.05 were considered statistically significant.

Results

$A\beta_{25–35}$ promotes cellular death in rBMVEC

The incubation of rBMEC with Aβ25–35 (20 μM) produces cellular death. Cytotoxicity was measured by MTT and LDH assays. $A\beta_{25–35}$ decreased cell viability by 27% compared to $A\beta_{35–25}$ (Fig. 1a), accompanied by an increase of 17% in LDH release (Fig. 1b). Control conditions (cell media) did not show any significant difference when comparing with Aβ35–25 (data not showed in the final figure), assuring that $A\beta_{35–25}$ is a suitable control condition to evaluate the effect of $A\beta_{25–35}$. Data represent values of three independent isolations ($N = 3$), student "t" test analysis, $^{**}p < 0.01$, $^{***}p < 0.001$. The data obtained by MTT and LDH support the use of $A\beta_{35–25}$ as a suitable control, from now on the rest of the experiment we did not include the control condition.

$A\beta_{25–35}$ produced oxidative stress in rBMVEC

The incubation of rBMEC with Aβ25–35 (20 μM) produces oxidative stress. $A\beta_{25–35}$ increased ROS production by 31% (Fig. 2a). The increase in ROS correlated with a 56% decrease in the expression of GPx1/2 (Fig. 2b). Data represent values of three independent experiments ($N = 3$), student "t" test analysis, $^{*}p < 0.05$, $^{***}p < 0.001$.

$A\beta_{25–35}$ exposure induces rBMVECs disruption

To establish whether the functionality of the BBB was compromised, TEER and FF across the rBMVEC monolayer were analyzed as indicators of BBB permeability. A significant decrease in TEER of 40.4 ± 8.8% was observed 24 h after

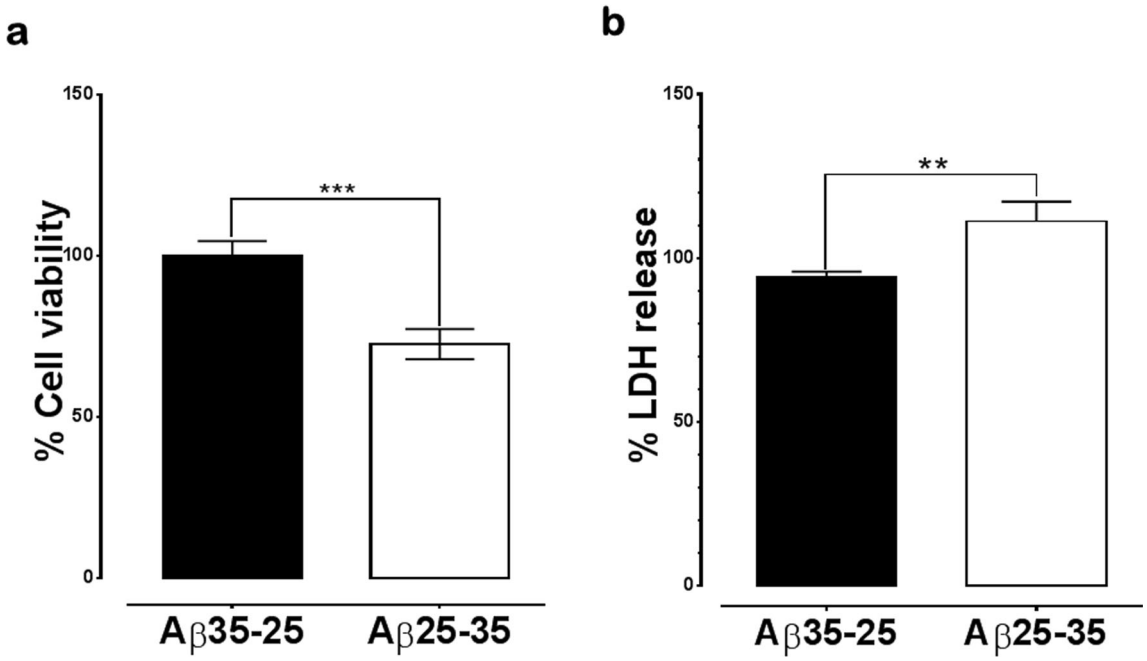

Fig. 1 $A\beta_{25–35}$ **produces rBMVEC toxicity. a** MTT assay and **b** LDH release. The evaluation was done in rBMVEC after 24-h exposure to $A\beta_{25–35}$ (white bars) or $A\beta_{35–25}$ (black bars, as the control group) at 20 μM. Values are expressed as mean ± SEM of $N = 3$ independent isolations. ***$p < 0.001$, **$p < 0.01$. *Student "t" test analysis*

exposure to 20 μM $A\beta_{25–35}$ (Fig. 3a). Consistent with this observation, a 50.8 ± 4.6% increase of FF across the rBMVEC monolayer was also detected (Fig. 3b). The decrease in TEER and increase in permeability is also accompanied with a decrease of 0.39 ± 0.119-fold in ZO-1 expression and an increase of 3.3 ± 1.62 fold in OC (Fig. 3c). Data represent values of three independent isolations (N = 3), student "t" test analysis, *p < 0.05, **$p < 0.01$, ***p < 0.001 ****$p < 0.0001$.

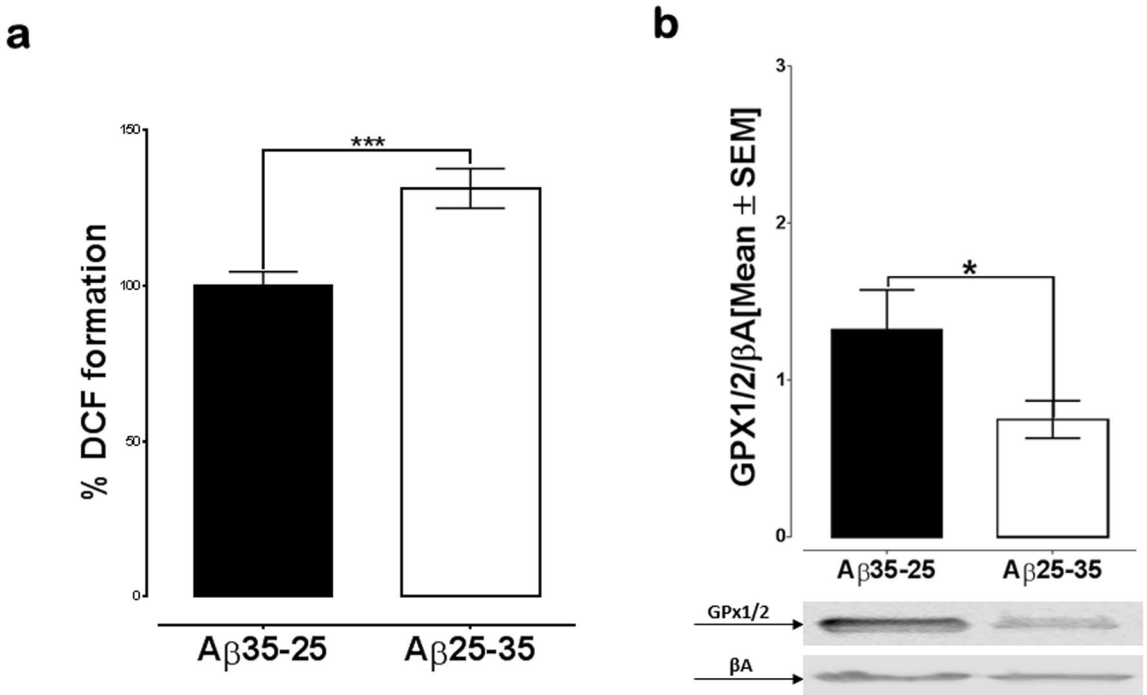

Fig. 2 $A\beta_{25–35}$ **produces cytotoxicity via OS. a** ROS production and **b** GPx1/2 levels. The evaluation was done in rBMVEC after 24-h exposure to $A\beta_{25–35}$ (white bars, solid line) or $A\beta_{35–25}$ (black bars, as the control group) at 20 μM. Representative bands are shown in B. Values are expressed as mean ± SEM of N = 3 independent isolations. ***$p < 0.001$, *$p < 0.05$. *Student "t" test analysis*

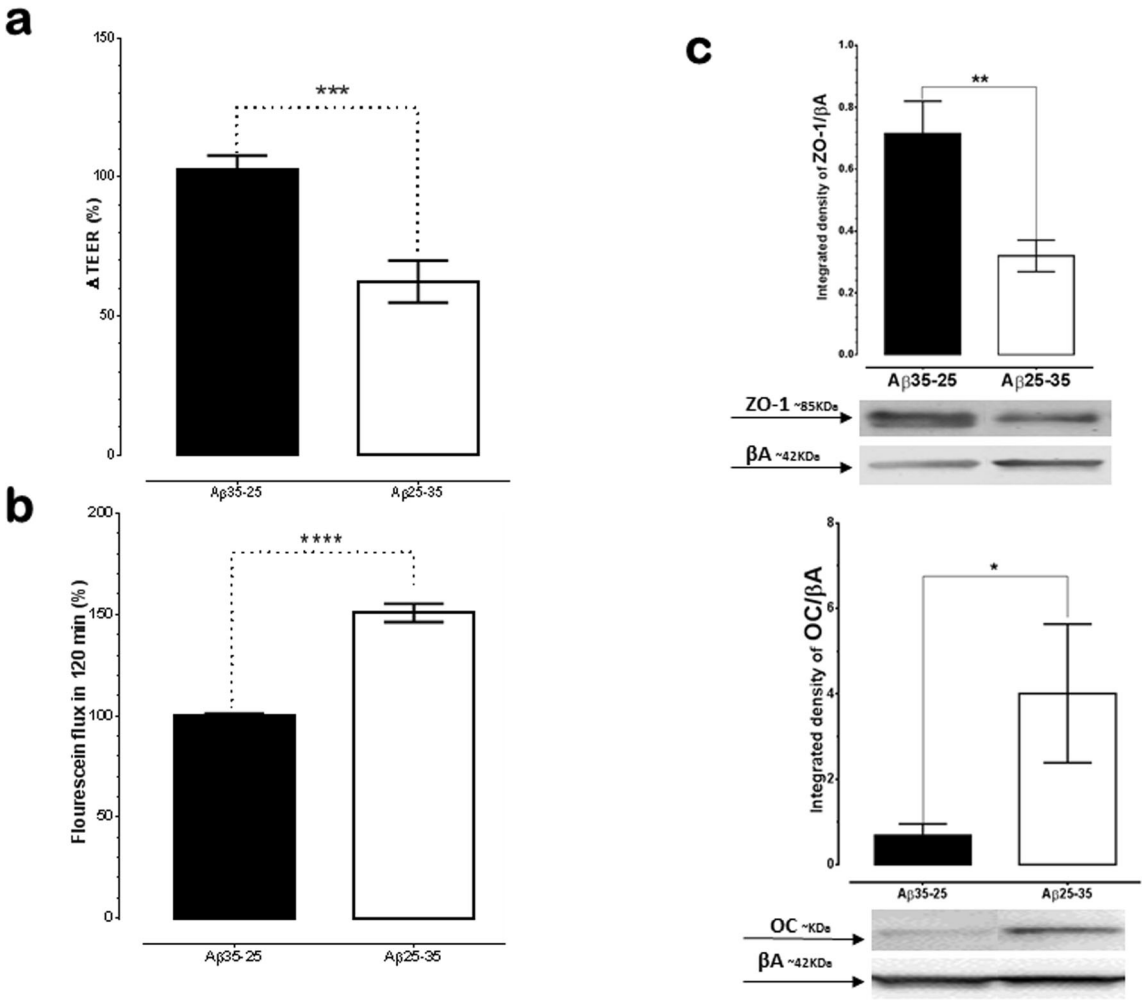

Fig. 3 $A\beta_{25–35}$ disrupts the rBMVEC monolayer and alters TJ expression. a TEER; **b** fluorescein flux and **c** ZO-1 and OC expression levels. The evaluation was done in rBMVEC after 24-h exposure to $A\beta_{25–35}$ (white bars, solid line) or $A\beta_{35–25}$ (black bars, as the control group) at 20 μM. Representative WB bands are shown in C. Values are expressed as mean ± SEM of N = 3 independent isolations. ****$p < 0.0001$, ***$p < 0.001$, **$p < 0.01$, *$p < 0.05$. *Student "t" test analysis*

$A\beta_{25–35}$ is producing morphological changes associated with the increase of RAGE expression

Significant morphological alterations in rBMVECs were observed 24 h after exposure to 20 μM $A\beta_{25–35}$ (Fig. 4a) including cellular disarrangement, loss of the rBMVEC monolayer and "cellular aggregation" (yellow arrow). To test the colocalization of Aβ-RAGE, these proteins were labeled by immunohistochemistry. The colocalization of Aβ-RAGE was observed in $A\beta_{25–35}$-treated rBMVECs, particularly at areas where cellular disarrangement was visible (Fig. 4b), suggesting the potential binding between them. However, further assays are needed to evidence the binding between $A\beta_{25–35}$ and RAGE. In addition to the colocalization, there was a significant increase of 84% and 66% in Aβ and RAGE labeling, respectively (Fig. 4c). Further quantification of RAGE was done by WB, which demonstrated an increase in RAGE level by 0.9 folds (Fig. 4d). Data represent values of three independent isolations ($N = 3$), student "t" test analysis, *$p < 0.05$, **$p < 0.01$.

Discussion

The findings in the present study demonstrate that $A\beta_{25–35}$ induces cytotoxicity by increasing OS and changing the expression of certain TJ proteins, compromising the morpho-functionality of the BBB in vitro. These events may potentially modulate the increase of RAGE expression/activation, initiating a vicious cycle of damage, in this particular in vitro model of the BBB. These data add credence to the hypothesis that abnormal RAGE activation may contribute to AD-related pathology.

Increased ROS production as a consequence of mitochondrial dysfunction is known to contribute cellular death to the

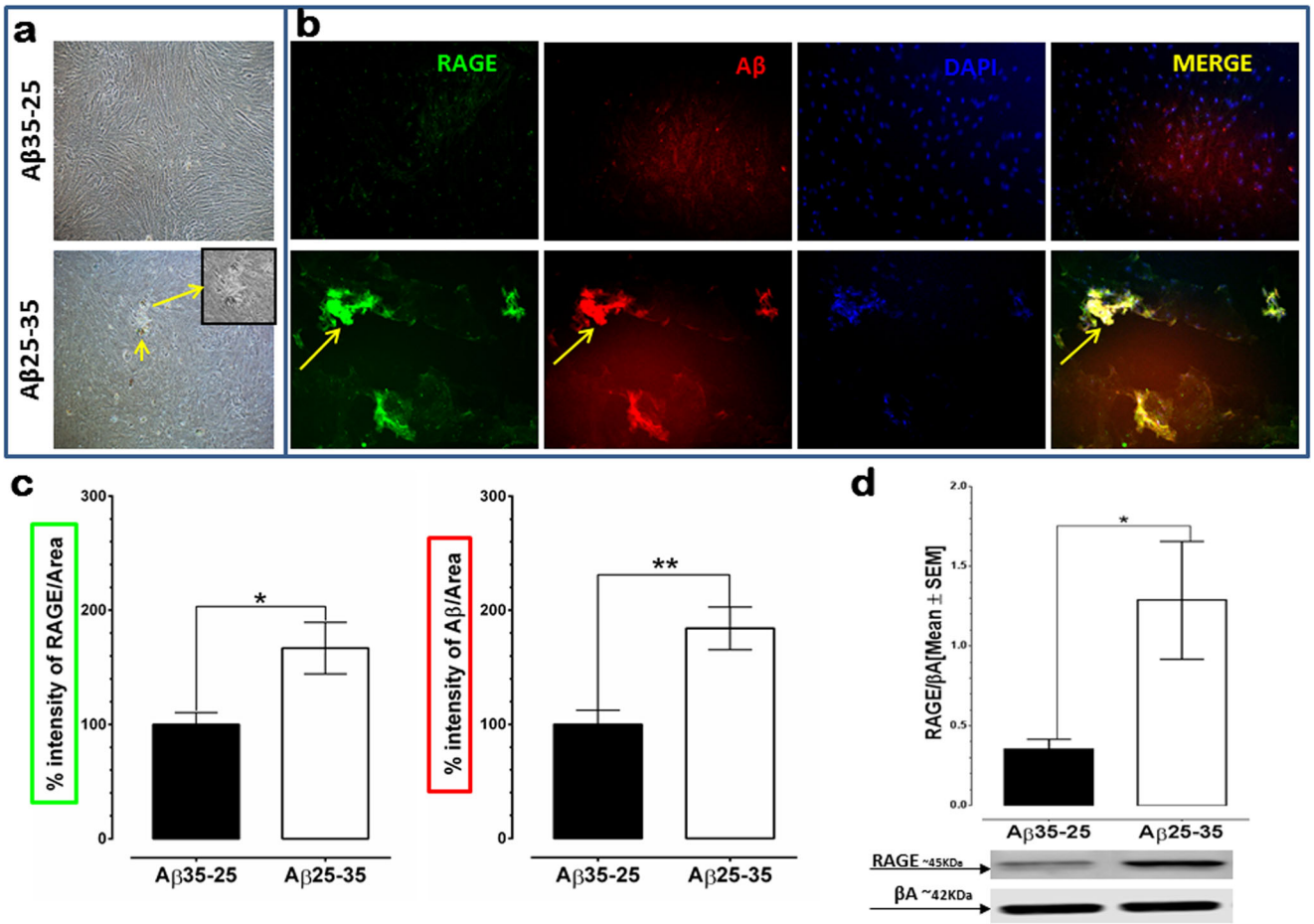

Fig. 4 $A\beta_{25–35}$ induces morphological changes, including Aβ-RAGE co-localization and RAGE upregulation. a Morphology of rBMVEC under bright field microscopy. Aggregations of rBMVEC indicated by yellow arrows. **b** Co-localization of RAGE (green) and Aβ (red) in fluorescent microscopy. Colocalization (yellow) is evident where cellular aggregation occurs. Representative images (10X) of $A\beta_{25–35}$ or $A\beta_{35–25}$ (as the control group) at 20 μM, ($n = 9$) were chosen. **c** Quantification of RAGE (green) and Aβ (red) labeling, Aβ25–35 (white bars) or Aβ35–25 (black bars, as the control group), **d** RAGE expression levels with representative WB bands shown. Values are expressed as mean ± SEM of $n = 3$ independent isolations. $^{**}p < 0.001$, $^{*}p < 0.05$. *Student "t" test analysis*

early stages of AD (Uttara et al. 2009). Moreover, it is known that $A\beta_{25–35}$ produces neurotoxicity in SH-SY5Y cells via oxidative stress (Liu et al. 2017b). However, little is investigated about the effects of $A\beta_{25–35}$ on the function of the BBB. In the present study, using rBMVECs as in vitro model of the BBB, we observed that 24 h exposure to $A\beta_{25–35}$ resulted in a significant decrease in cell viability and induced cellular toxicity when compared to the $A\beta_{35–25}$ (mimic control condition), the cytotoxicity produced by $A\beta_{25–35}$ has been previously demonstrated in differentiated PC12 cells (Xu et al. 2016). This effect co-occurred with an increase in ROS production and a decrease in GPx1/2 expression. This relationship indicates that OS may play a role in the toxic effects of $A\beta_{25–35}$ in rBMVEC. These results agree with previous in vitro and in vivo studies where $A\beta_{25–35}$ promoted neurotoxicity by increasing OS; these toxic effects were prevented by the presumed antioxidant capacities of triptolides (Xu et al. 2016), flavonoids (Cuevas et al. 2009; Guimaraes et al. 2015), estradiol (Bernal-Mondragon et al. 2013), and s-allyl-cysteine (Perez-Severiano et al. 2004), suggesting indirectly that $A\beta_{25–35}$ generates OS in neurons. In the human cerebral microvascular endothelial cell line (HCMEC/D3), ROS production was increased after exposure to the full-length Aβ ($A\beta_{1–42}$), which could be prevented by co-treatment with an antioxidant (Carrano et al. 2011). Moreover, $A\beta_{1–42}$ has been shown to induce apoptosis in a ROS mediated fashion in a murine brain capillary endothelial cell line (bEnd.3) (Wan et al. 2014a, b), supporting the hypothesis that Aβ produces oxidative stress in the cells of the BBB in a similar manner as in neurons.

OS is thought trigger BBB disruption which will result in increase of permeability. There are multiples mechanism by which this could occur but the most likely is the reorganization of TJs (Lochhead et al. 2010; Blasig et al. 2011). In this context, we observed that $A\beta_{25–35}$ decreased the TEER and increased barrier permeability across the rBMVEC monolayer, as indicated by increased FF. These effects were concomitant

with a decrease in the expression of ZO-1 and an increase in the expression of OC. The changes in protein expression may be the result of the observed increase in paracellular permeability. While this is the first study documenting the effects of $A\beta_{25–35}$ on the integrity and TJs changes of the rBMVEC, previous studies using different Aβ peptides have been published and support the effect we found. For instance, the fibrillary form $A\beta_{1–40}$ at a concentration of 20 μM decreased the TEER and increase the FF in an in vitro model of the BBB consisting of co-cultures of human BMVEC (hBMVEC) and human astrocytes (hAs) (Zhang et al. 2017). In the HCMEC/D3 cell line, a combination of $A\beta_{1–42}$ and $A\beta_{1–40}$ increased the paracellular permeability, which was attributed to alteration in the clearance and deposition of Aβ as a result of downregulation of LRP-1 and up-regulation in RAGE (Qosa et al. 2014). The same group later suggested that $A\beta_{1–42}$ induced BBB disruption by upregulation of RAGE and metalloproteinases as well as a decrease in the expression of TJ proteins (Wan et al. 2015). Regarding the changes in TJSs, previous studies have reported that intraventricular injection of $A\beta_{25–35}$ induces down-regulation of ZO-1, OC, and C-5 after 8 days in a murine model; suggesting possible chronic neurovascular damage (Liu et al. 2009). In agree with these reports, we found ZO1 decreased. Surprisingly, we found that rBMVEC after 24 h of Aβ25–35 treatment produced an increase of OC levels. Little is known about the role of BBB on each specific TJ during the progression of AD. The changes in TJs in models of Aβ-induced neurotoxicity are not well characterized. Previous studies using BBB models have reported the increase of OC as a transitory response. In MDCK cells, Aβ1–42 increased OC levels 24 h after exposure of (Gheorghiu et al. 2014). Similarly, an increase in OC expression in CMEC/D3 cells has been observed 24 h after exposure, suggesting an attempt of compensate for the Aβ1–42-induced acute toxicity (Paik et al. 2018). In addition, a separate study using hCMEC/D3 cells exposed to Aβ1–40, indicates that OC levels were slightly increased after 24 h of treatment, but after 48 h of exposure the decrease of OC was significant. Claudin-5 and ZO-1 did not show any changes under this condition Likewise, we can speculate the Aβ25–35 increases OC levels due to acute toxicity, as a prevention response of the BBB dysfunction and may be a transient effect. Further studies are warranty to track these possibilities.

It has been previously demonstrated that interaction of $A\beta_{1–42}$ with RAGE induces downregulation and structural alteration of ZO-1, and increases paracellular permeability in bEnd.3 cells. Treatment with anti-RAGE antibodies blocked these effects, suggesting the participation of RAGE in Aβ-induced microvascular toxicity (Kook et al. 2012). A neuropathological study has shown a positive correlation between RAGE expression and plaque burden in humans, indicating a role of RAGE and altered BBB function in the formation of plaques and subsequent pathogenesis of AD (Provias and Jeynes 2014). Furthermore, we also show that RAGE expression was increased at sites of cellular disarrangement and co-localized with Aβ. Previous studies have shown that RAGE is highly expressed in the hippocampal micro-vasculature in patients with AD (Donahue et al. 2006; Carrano et al. 2011) which may contribute to the deposition of Aβ in the brain as well as the formation of senile plaques (Provias and Jeynes 2014). Inhibition of RAGE has been documented to decrease Aβ-induced toxicity in a mouse model (Deane et al. 2012), as well as decrease transport of Aβ through the BBB, diminishing its accumulation in the brain (Deane et al. 2003) thereby ameliorating cognitive impairment and promoting hippocampal plasticity (Wang et al. 2018). The significant increase of RAGE levels, presented here, after $A\beta_{25–35}$ exposure in rBMVECs, supports previous findings using different Aβ peptides, suggesting a common mechanism of action of Aβ peptides on BBB models, making $A\beta_{25–35}$ a suitable tool to do research in AD field.

In summary, our data suggest that $A\beta_{25–35}$ induces BBB dysfunction in vitro, which is likely mediated by OS and ultimately leads to disruption of BBB integrity and cell death. Based in previous findings we can suggest that these changes could potentially be mediated by RAGE, possibly by either mediating excessive ROS production and/or the interaction with $A\beta_{25–35}$, however, this molecular interaction remains uncertain. The possible interactions may lead to the formation of plaque-like structures in the regions of high RAGE expression. The exact molecular pathway(s) that are activated as a result of this unique interaction requires further investigation, as well.

Acknowledgements These studies were supported by FDA/NCTR, E0763101, and postdoctoral fellowships from the Oak Ridge Institute for Science and Education through an interagency agreement between the US Department of Energy and the FDA (to E. Cuevas). The authors are grateful to John Talpos for support in preparing this manuscript.

The views and the information in this article is solely the responsibility of the authors and is not a formal dissemination of information by the U.S. Food and Drug Administration and does not represent agency position or policy.

Compliance with ethical standards

Conflict of interest The authors declare no conflict of interest.

References

Alzheimer's A (2016) 2016 Alzheimer's disease facts and figures. Alzheimers Dement 12(4):459–509

Bednarczyk J, Lukasiuk K (2011) Tight junctions in neurological diseases. Acta Neurobiol Exp (Wars) 71(4):393–408

Bernal-Mondragon C, Rivas-Arancibia S, Kendrick KM, Guevara-Guzman R (2013) Estradiol prevents olfactory dysfunction induced by A-beta 25-35 injection in hippocampus. BMC Neurosci 14:104

Blasig IE, Bellmann C, Cording J, Del Vecchio G, Zwanziger D, Huber O, Haseloff RF (2011) Occludin protein family: oxidative stress and reducing conditions. Antioxid Redox Signal 15(5):1195–1219

Butterfield DA, Kanski J (2002) Methionine residue 35 is critical for the oxidative stress and neurotoxic properties of Alzheimer's amyloid beta-peptide 1-42. Peptides 23(7):1299–1309

Carrano A, Hoozemans JJ, van der Vies SM, Rozemuller AJ, van Horssen J, de Vries HE (2011) Amyloid Beta induces oxidative stress-mediated blood-brain barrier changes in capillary amyloid angiopathy. Antioxid Redox Signal 15(5):1167–1178

Chaney MO, Stine WB, Kokjohn TA, Kuo YM, Esh C, Rahman A, Luehrs DC, Schmidt AM, Stern D, Yan SD, Roher AE (2005) RAGE and amyloid beta interactions: atomic force microscopy and molecular modeling. Biochim Biophys Acta 1741(1–2): 199–205

Cuevas E, Limon D, Perez-Severiano F, Diaz A, Ortega L, Zenteno E, Guevara J (2009) Antioxidant effects of Epicatechin on the hippocampal toxicity caused by amyloid-beta 25-35 in rats. Eur J Pharmacol 616(1–3):122–127

Cuevas E, Lantz S, Newport G, Divine B, Wu Q, Paule MG, Tobon-Velasco JC, Ali SF, Santamaria A (2010) On the early toxic effect of quinolinic acid: involvement of RAGE. Neurosci Lett 474(2):74–78

Cuevas E, Lantz SM, Tobon-Velasco JC, Newport GD, Wu Q, Virmani A, Ali SF, Santamaria A (2011) On the in vivo early toxic properties of A-beta 25-35 peptide in the rat hippocampus: involvement of the receptor-for-advanced glycation-end-products and changes in gene expression. Neurotoxicol Teratol 33(2):288–296

Deane RJ (2012) Is RAGE still a therapeutic target for Alzheimer's disease? Future Med Chem 4(7):915–925

Deane R, Zlokovic BV (2007) Role of the blood-brain barrier in the pathogenesis of Alzheimer's disease. Curr Alzheimer Res 4(2): 191–197

Deane R, Du Yan S, Submamaryan RK, LaRue B, Jovanovic S, Hogg E, Welch D, Manness L, Lin C, Yu J, Zhu H, Ghiso J, Frangione B, Stern A, Schmidt AM, Armstrong DL, Arnold B, Liliensiek B, Nawroth P, Hofman F, Kindy M, Stern D, Zlokovic B (2003) RAGE mediates amyloid-beta peptide transport across the blood-brain barrier and accumulation in brain. Nat Med 9(7):907–913

Deane R, Wu Z, Zlokovic BV (2004) RAGE (yin) versus LRP (yang) balance regulates alzheimer amyloid beta-peptide clearance through transport across the blood-brain barrier. Stroke 35(11 Suppl 1): 2628–2631

Deane R, Singh I, Sagare AP, Bell RD, Ross NT, LaRue B, Love R, Perry S, Paquette N, Deane RJ, Thiyagarajan M, Zarcone T, Fritz G, Friedman AE, Miller BL, Zlokovic BV (2012) A multimodal RAGE-specific inhibitor reduces amyloid beta-mediated brain disorder in a mouse model of Alzheimer disease. J Clin Invest 122(4): 1377–1392

Denizot F, Lang R (1986) Rapid colorimetric assay for cell-growth and survival - modifications to the tetrazolium dye procedure giving improved sensitivity and reliability. J Immunol Methods 89(2): 271–277

Do TM, Dodacki A, Alata W, Calon F, Nicolic S, Scherrmann JM, Farinotti R, Bourasset F (2016) Age-dependent regulation of the blood-brain barrier influx/efflux equilibrium of amyloid-beta peptide in a mouse model of Alzheimer's disease (3xTg-AD). J Alzheimers Dis 49(2):287–300

Donahue JE, Flaherty SL, Johanson CE, Duncan JA 3rd, Silverberg GD, Miller MC, Tavares R, Yang W, Wu Q, Sabo E, Hovanesian V, Stopa EG (2006) RAGE, LRP-1, and amyloid-beta protein in Alzheimer's disease. Acta Neuropathol 112(4):405–415

Fanning AS, Jameson BJ, Jesaitis LA, Anderson JM (1998) The tight junction protein ZO-1 establishes a link between the transmembrane protein occludin and the actin cytoskeleton. J Biol Chem 273(45): 29745–29753

Frozza RL, Horn AP, Hoppe JB, Simao F, Gerhardt D, Comiran RA, Salbego CG (2009) A comparative study of beta-amyloid peptides Abeta1-42 and Abeta25-35 toxicity in organotypic hippocampal slice cultures. Neurochem Res 34(2):295–303

Gheorghiu M, Enciu AM, Popescu BO, Gheorghiu E (2014) Functional and molecular characterization of the effect of amyloid-beta42 on an in vitro epithelial barrier model. J Alzheimers Dis 38(4):787–798

Gospodarska E, Kupniewska-Kozak A, Goch G, Dadlez M (2011) Binding studies of truncated variants of the Abeta peptide to the V-domain of the RAGE receptor reveal Abeta residues responsible for binding. Biochim Biophys Acta 1814(5):592–609

Guimaraes CC, Oliveira DD, Valdevite M, Saltoratto AL, Pereira SI, Franca Sde C, Pereira AM, Pereira PS (2015) The glycosylated flavonoids vitexin, isovitexin, and quercetrin isolated from Serjania erecta Radlk (Sapindaceae) leaves protect PC12 cells against amyloid-beta25-35 peptide-induced toxicity. Food Chem Toxicol 86:88–94

Hardy J, Allsop D (1991) Amyloid deposition as the central event in the aetiology of Alzheimer's disease. Trends Pharmacol Sci 12(10): 383–388

Hardy J, Selkoe DJ (2002) The amyloid hypothesis of Alzheimer's disease: progress and problems on the road to therapeutics. Science 297(5580):353–356

Kook SY, Hong HS, Moon M, Ha CM, Chang S, Mook-Jung I (2012) Abeta(1)(−)(4)(2)-RAGE interaction disrupts tight junctions of the blood-brain barrier via ca(2)(+)-calcineurin signaling. J Neurosci 32(26):8845–8854

Kubo T, Nishimura S, Kumagae Y, Kaneko I (2002) In vivo conversion of racemized beta-amyloid ([D-Ser 26]A beta 1-40) to truncated and toxic fragments ([D-Ser 26]A beta 25-35/40) and fragment presence in the brains of Alzheimer's patients. J Neurosci Res 70:474–483

Liu R, Gao M, Qiang GF, Zhang TT, Lan X, Ying J, Du GH (2009) The anti-amnesic effects of luteolin against amyloid beta(25-35) peptide-induced toxicity in mice involve the protection of neurovascular unit. Neuroscience 162(4):1232–1243

Liu T, Liu WH, Zhao JS, Meng FZ, Wang H (2017a) Lutein protects against beta-amyloid peptide-induced oxidative stress in cerebrovascular endothelial cells through modulation of Nrf-2 and NF-kappab. Cell Biol Toxicol 33(1):57–67

Liu XY, Zhang LJ, Chen Z, Liu LB (2017b) The PTEN inhibitor bpV(pic) promotes neuroprotection against amyloid beta-peptide (25-35)-induced oxidative stress and neurotoxicity. Neurol Res 39(8):758–765

Lochhead JJ, McCaffrey G, Quigley CE, Finch J, DeMarco KM, Nametz N, Davis TP (2010) Oxidative stress increases blood-brain barrier permeability and induces alterations in occludin during hypoxia-reoxygenation. J Cereb Blood Flow Metab 30(9):1625–1636

Mackic JB, Stins M, McComb JG, Calero M, Ghiso J, Kim KS, Yan SD, Stern D, Schmidt AM, Frangione B, Zlokovic BV (1998) Human blood-brain barrier receptors for Alzheimer's amyloid-beta 1- 40. Asymmetrical binding, endocytosis, and transcytosis at the apical side of brain microvascular endothelial cell monolayer. J Clin Invest 102(4):734–743

Mark KS, Davis TP (2002) Cerebral microvascular changes in permeability and tight junctions induced by hypoxia-reoxygenation. Am J Physiol Heart Circ Physiol 282(4):H1485–H1494

Mawuenyega KG, Sigurdson W, Ovod V, Munsell L, Kasten T, Morris JC, Yarasheski KE, Bateman RJ (2010) Decreased clearance of CNS beta-amyloid in Alzheimer's disease. Science 330(6012):1774

Millucci L, Ghezzi L, Bernardini G, Santucci A (2010) Conformations and biological activities of amyloid beta peptide 25-35. Curr Protein Pept Sci 11:54–67

Paik S, Somvanshi RK, Kumar U (2018) Somatostatin maintains permeability and integrity of blood-brain barrier in beta-amyloid induced toxicity. Mol Neurobiol

Park S, Kim DS, Kang S, Moon NR (2013) Beta-amyloid-induced cognitive dysfunction impairs glucose homeostasis by increasing

insulin resistance and decreasing beta-cell mass in non-diabetic and diabetic rats. Metabolism 62(12):1749–1760

Perez-Severiano F, Salvatierra-Sanchez R, Rodriguez-Perez M, Cuevas-Martinez EY, Guevara J, Limon D, Maldonado PD, Medina-Campos ON, Pedraza-Chaverri J, Santamaria A (2004) S-allylcysteine prevents amyloid-beta peptide-induced oxidative stress in rat hippocampus and ameliorates learning deficits. Eur J Pharmacol 489(3):197–202

Pike CJ, Burdick D, Walencewicz AJ, Glabe CG, Cotman CW (1993) Neurodegeneration induced by beta-amyloid peptides in vitro: the role of peptide assembly state. J Neurosci 13(4):1676–1687

Pike CJ, Walencewicz-Wasserman AJ, Kosmoski J, Cribbs DH, Glabe CG, Cotman CW (1995) Structure-activity analyses of beta-amyloid peptides: contributions of the beta 25-35 region to aggregation and neurotoxicity. J Neurochem 64(1):253–265

Provias J, Jeynes B (2014) The role of the blood-brain barrier in the pathogenesis of senile plaques in Alzheimer's disease. Int J Alzheimers Dis 2014:191863

Qosa H, LeVine H 3rd, Keller JN, Kaddoumi A (2014) Mixed oligomers and monomeric amyloid-beta disrupts endothelial cells integrity and reduces monomeric amyloid-beta transport across hCMEC/D3 cell line as an in vitro blood-brain barrier model. Biochim Biophys Acta 1842(9):1806–1815

Rosas-Hernandez H, Cuevas E, Lantz SM, Hamilton WR, Ramirez-Lee MA, Ali SF, Gonzalez C (2013a) Prolactin and blood-brain barrier permeability. Curr Neurovasc Res 10(4):278–286

Rosas-Hernandez H, Cuevas E, Lantz-McPeak SM, Ali SF, Gonzalez C (2013b) Prolactin protects against the methamphetamine-induced cerebral vascular toxicity. Curr Neurovasc Res 10(4):346–355

Rosas-Hernandez H, Cuevas E, Escudero-Lourdes C, Lantz SM, Sturdivant NM, Imam SZ, Sarkar S, Slikker W Jr, Paule MG, Balachandran K, Ali SF (2018a) Characterization of uniaxial high-speed stretch as an in vitro model of mild traumatic brain injury on the blood-brain barrier. Neurosci Lett 672:123–129

Rosas-Hernandez H, Cuevas E, Lantz SM, Paule MG, Ali SF (2018b) Isolation and culture of brain microvascular endothelial cells for in vitro blood-brain barrier studies. Methods Mol Biol 1727:315–331

Self RL, Smith KJ, Mulholland PJ, Prendergast MA (2005) Ethanol exposure and withdrawal sensitizes the rat hippocampal CA1 pyramidal cell region to beta-amyloid (25-35)-induced cytotoxicity: NMDA receptor involvement. Alcohol Clin Exp Res 29(11): 2063–2069

Selkoe DJ, Hardy J (2016) The amyloid hypothesis of Alzheimer's disease at 25 years. EMBO Mol Med 8:595–608

Steinerman JR, Irizarry M, Scarmeas N, Raju S, Brandt J, Albert M, Blacker D, Hyman B, Stern Y (2008) Distinct pools of beta-amyloid in Alzheimer disease-affected brain: a clinicopathologic study. Arch Neurol 65(7):906–912

Stepanichev MY, Moiseeva YV, Lazareva NA, Onufriev MV, Gulyaeva NV (2010) Changes in cell proliferation in the subventricular zone of the brain in adult rats given beta-amyloid peptide (25-35). Neurosci Behav Physiol 40(2):123–126

Strazielle N, Ghersi-Egea JF, Ghiso J, Dehouck MP, Frangione B, Patlak C, Fenstermacher J, Gorevic P (2000) In vitro evidence that beta-amyloid peptide 1-40 diffuses across the blood-brain barrier and affects its permeability. J Neuropathol Exp Neurol 59(1):29–38

Thal DR, Rub U, Orantes M, Braak H (2002) Phases of a beta-deposition in the human brain and its relevance for the development of AD. Neurology 58(12):1791–1800

Uttara B, Singh AV, Zamboni P, Mahajan RT (2009) Oxidative stress and neurodegenerative diseases: a review of upstream and downstream antioxidant therapeutic options. Curr Neuropharmacol 7(1):65–74

Wan WB, Cao L, Liu LM, Kalionis B, Chen C, Tai XT, Li YM, Xia SJ (2014a) EGb761 provides a protective effect against Abeta1-42 oligomer-induced cell damage and blood-brain barrier disruption in an in vitro bEnd.3 endothelial model. PLoS One 9(11):e113126

Wan W, Chen H, Li Y (2014b) The potential mechanisms of Abeta-receptor for advanced glycation end-products interaction disrupting tight junctions of the blood-brain barrier in Alzheimer's disease. Int J Neurosci 124(2):75–81

Wan W, Cao L, Liu L, Zhang C, Kalionis B, Tai X, Li Y, Xia S (2015) Abeta(1-42) oligomer-induced leakage in an in vitro blood-brain barrier model is associated with up-regulation of RAGE and metalloproteinases, and down-regulation of tight junction scaffold proteins. J Neurochem 134(2):382–393

Wang H, Joseph JA (1999) Quantifying cellular oxidative stress by dichlorofluorescein assay using microplate reader. Free Radic Biol Med 27(5–6):612–616

Wang H, Chen F, Du YF, Long Y, Reed MN, Hu M, Suppiramaniam V, Hong H, Tang SS (2018) Targeted inhibition of RAGE reduces amyloid-beta influx across the blood-brain barrier and improves cognitive deficits in db/db mice. Neuropharmacology 131:143–153

Watson PM, Anderson JM, Vanltallie CM, Doctrow SR (1991) The tight-junction-specific protein ZO-1 is a component of the human and rat blood-brain barriers. Neurosci Lett 129(1):6–10

Weller RO, Subash M, Preston SD, Mazanti I, Carare RO (2008) Perivascular drainage of amyloid-beta peptides from the brain and its failure in cerebral amyloid angiopathy and Alzheimer's disease. Brain Pathol 18(2):253–266

Xie J, Reverdatto S, Frolov A, Hoffmann R, Burz DS, Shekhtman A (2008) Structural basis for pattern recognition by the receptor for advanced glycation end products (RAGE). J Biol Chem 283(40): 27255–27269

Xu P, Wang H, Li Z, Yang Z (2016) Triptolide attenuated injury via inhibiting oxidative stress in amyloid-Beta25-35-treated differentiated PC12 cells. Life Sci 145:19–26

Yan SD, Chen X, Fu J, Chen M, Godman G, Stern D, Schmidt AM (1996a) RAGE: a receptor upregulated in Alzheimer's disease on neurons, microglia, and cerebrovascular endothelium that binds amyloid-beta peptide and mediates induction of oxidant stress. Neurology 46(2):23005–23005

Yan SD, Chen X, Fu J, Chen M, Zhu H, Roher A, Slattery T, Zhao L, Nagashima M, Morser J, Migheli A, Nawroth P, Stern D, Schmidt AM (1996b) RAGE and amyloid-beta peptide neurotoxicity in Alzheimer's disease. Nature 382(6593):685–691

Yankner BA, Duffy LK, Kirschner DA (1990) Neurotrophic and neurotoxic effects of amyloid beta protein: reversal by tachykinin neuropeptides. Science 250(4978):279–282

Zhang JX, Xing JG, Wang LL, Jiang HL, Guo SL, Liu R (2017) Luteolin inhibits fibrillary beta-Amyloid1-40-induced inflammation in a human blood-brain barrier model by suppressing the p38 MAPK-mediated NF-kappaB signaling pathways. Molecules 22(3)

Zheng X, Xie Z, Zhu Z, Liu Z, Wang Y, Wei L, Yang H, Yang H, Liu Y, Bi J (2014) Methyllycaconitine alleviates amyloid-beta peptides-induced cytotoxicity in SH-SY5Y cells. PLoS One 9(10):e111536

Zlokovic BV (2011) Neurovascular pathways to neurodegeneration in Alzheimer's disease and other disorders. Nat Rev Neurosci 12(12): 723–738